Published in final edited form as:
Osteoarthritis Cartilage. 2012 November ; 20(11): 1268–1277. doi:10.1016/j.joca.2012.07.016.

STRUCTURE-FUNCTION RELATIONSHIPS IN OSTEOARTHRITIC HUMAN HIP JOINT ARTICULAR CARTILAGE

Janne T.A. Mäkelä, M.Sc.[1,2], **Mari R.J. Huttu, B.Sc.**[1], and **Rami K. Korhonen, Ph.D**[1]

[1]Department of Applied Physics, University of Eastern Finland, POB 1627, FI-70211 Kuopio, Finland [2]Department of Clinical Physiology and Nuclear medicine, Kuopio University Hospital, POB 1777, FI-70211 Kuopio, Finland

Abstract

Objectives—It is currently poorly known how different structural and compositional components in human articular cartilage are related to their specific functional properties at different stages of osteoarthritis (OA). The objective of this study was to characterize the structure-function relationships of articular cartilage obtained from osteoarthritic human hip joints.

Methods—Articular cartilage samples with their subchondral bone ($n = 15$) were harvested during hip replacement surgeries from human femoral necks. Stress-relaxation tests, Mankin scoring, spectroscopic and microscopic methods were used to determine the biomechanical properties, OA grade, and the composition and structure of the samples. In order to obtain the mechanical material parameters for the samples, a fibril-reinforced poroviscoelastic model was fitted to the experimental data obtained from the stress-relaxation experiments.

Results—The strain-dependent collagen network modulus (E_f^{ε}) and the collagen orientation angle exhibited a negative linear correlation ($r = -0.65$, $p < 0.01$), while the permeability strain-dependency factor (M) and the collagen content exhibited a positive linear correlation ($r = 0.56$, $p < 0.05$). The non-fibrillar matrix modulus (E_{nf}) also exhibited a positive linear correlation with the proteoglycan content ($r = 0.54$, $p < 0.05$).

Conclusion—The study suggests that increased collagen orientation angle during OA primarily impairs the collagen network and the tensile stiffness of cartilage in a strain-dependent manner, while the decreased collagen content in OA facilitates fluid flow out of the tissue especially at high compressive strains. Thus, the results provide interesting and important information of the structure-function relationships of human hip joint cartilage and mechanisms during the progression of OA.

Keywords

Articular Cartilage; Osteoarthritis; Collagen; Proteoglycans; Fourier transform infrared imaging; Polarized light microscopy; Finite element analysis; Fibril reinforced

Correspondence: Janne Mäkelä, Department of Applied Physics, University of Eastern Finland, Yliopistonranta 1, POB 1627, 70211 Kuopio. Tel: +358 44 020 4034, Janne.Makela@uef.fi.

CONTRIBUTIONS

All authors have contributed to the conception and design of the study, and acquisition, analysis and interpretation of data. The manuscript has been drafted, revised and finally approved by all authors. Mäkelä JTA (Janne.Makela@uef.fi) takes responsibility for the integrity of the work.

CONFLICT OF INTEREST

Authors have no conflicts of interest.

Europe PMC Funders Author Manuscripts

INTRODUCTION

The mechanical properties of articular cartilage are determined by the content, arrangement and interactions of the tissue constituents, *i.e.*, the three-dimensional collagen network, proteoglycans (PGs) and interstitial water[1]. The interstitial fluid pressure contributes strongly to the tissue stiffness under instant loads. However, under prolonged loads, fluid flows out of the tissue and PGs are mainly responsible for the tissue's compressive (equilibrium) stiffness. Collagen fibers determine the tensile properties of articular cartilage. In osteoarthritis (OA), there are several alterations in these constituents that lead to changes in the mechanical properties of cartilage; reduction of PG and collagen content, collagen fibrillation (especially in the superficial zone of articular cartilage) and an increase in the fluid content[2-9]. These alterations in structure and composition lead to increased permeability, allowing water to flow out of the tissue faster, and the decreased equilibrium and dynamic mechanical stiffness of articular cartilage.

Even though structural and compositional changes are known to occur in OA, it is not fully understood how different components in cartilage are related to their functional properties at different stages of OA. Specifically, the biomechanical properties of articular cartilage and their relationships with the structure and composition, especially in the human hip joint, are poorly known. Instead, many studies of articular cartilage and OA progression are based on animal models[10-12]. Furthermore, most of the studies investigating structure-function relationships of cartilage[13-15] have applied microscopic, spectroscopic and biomechanical methods for the characterization of collagen and PG content, collagen orientation, and tissue mechanical stiffness. However, these studies have not utilized computational models in order to obtain more specific mechanical properties for the collagen network, PGs and fluid.

There are many computational models that have been developed and applied to characterize the mechanical properties and behavior of articular cartilage[16-19], but the fibril-reinforced biphasic models are able to separate the mechanical effects of collagen, PGs and fluid in loaded articular cartilage[4,18,20-24]. In the fibril reinforced models, the nonfibrillar matrix and fibril network moduli describe the mechanical effects of PGs and collagen, while the permeability can be used to characterize fluid flow and its changes along with alterations in void ratio during tissue compression.

The purpose of this study was to characterize the fibril reinforced biphasic material properties of articular cartilage from osteoarthritic human hip joints and to investigate their relationships with tissue structure and composition. For these aims, microscopic and spectroscopic methods were used to analyze the composition and structure, *i.e.*, collagen and PG content and collagen orientation of the samples, and the biomechanical tests with computational modeling were applied to resolve the mechanical properties of the samples, specifically permeability, fibril network modulus and nonfibrillar matrix modulus. This study provides novel information of the constituent specific functional properties of osteoarthritic human articular cartilage, and the structure-function relationships of cartilage during the progression of hip joint OA.

METHODS

STUDY PROTOCOL

Articular cartilage samples with subchondral bone (n = 15, from 9 patients, diameter =18 mm) were harvested from random locations in human femoral heads during the hip replacement operations. The samples were collected with the permission from the National Agency for Medicolegal Affairs in Finland (permission 103/13/03/02/09). Samples were stored in DMEM (1 g/l D-glucose, L-glutamine- and phenol red-free, Invitrogen, Paisley,

Europe PMC Funders Author Manuscripts

UK) supplemented with 100 U/ml of penicillin, 100 μg/ml of streptomycin (EuroClone S.p.A, Pavia, Italy) and 2.50 μg/ml Fungizone (amphotericin-B) (Invitrogen, Paisley, UK) in the incubator (37°C) for 24 or 48 hours before mechanical testing.

Biomechanical stress-relaxation tests were conducted for the samples and the fibril reinforced poroviscoelastic (FRPVE) finite element model was fitted to the experimental curves. Material parameters of the cartilage samples were obtained through optimization. After the biomechanical tests, the samples were processed for microscopy and spectroscopy. Spectroscopic and microscopic methods were used to determine the composition and structure of the cartilage samples; Fourier Transform-InfraRed Imaging (FTIRI) was used to measure the collagen content[3,6,25,26], digital densitometry (DD) was used to measure the PG content[27,28] and polarized light microscopy (PLM) was used to analyze the collagen orientation angles[29,30] of the samples. Every sample was also given a Mankin score to represent the severity of OA[31,32]. More details of each method is presented in the following subsections.

BIOMECHANICAL TESTING

Biomechanical stress-relaxation tests were conducted on the cartilage-on-bone samples using a flat-ended indenter (1.19 mm diameter). Thickness of the samples was first measured using a high resolution ultrasound system[33,34] (Clear View Ultra, Boston Scientific Corporation, San Jose, CA, USA). The samples were then glued on the bottom of the measuring chamber, which was then filled with Phosphate Buffered Saline (PBS). The indenter was driven into contact with the sample surface, after which the sample was allowed to relax for ~15 min. Then stepwise stress-relaxation tests with four steps in total, followed by a 900 s of relaxation, were applied with a ramp rate of 100 %/s and a step size of 5% of the cartilage thickness (Fig. 1). Our preliminary tests indicated that 900 s should be enough to reach the equilibrium. It was also consistent with the literature[21,35-37]. After biomechanical tests, the samples were fixed in formalin.

FRPVE MODEL AND SIMULATIONS

In order to obtain optimized values of the material parameters, the FRPVE model was fitted to the experimental biomechanical measurements using Abaqus (V6.10, Dassault Systèmes Simulia Corp., Providence, RI) and Matlab (V7.10.0, The MathWorks, Inc., Natick, MA) (Fig. 1). In the FRPVE model, articular cartilage consisted of a viscoelastic fibrillar matrix and a biphasic poroelastic, non-fibrillar matrix. The fibrillar part represented the collagen network, while the non-fibrillar part represented the proteoglycans with a porous structure filled with fluid. In order to keep the modeling analysis independent of the microscopic analysis in correlation analysis between the mechanical and structural parameters, the FRPVE model was assumed to be fully homogeneous through the tissue depth, similarly as in Li et al. (1999)[18] and Korhonen et al. (2003)[4].

In the FRPVE model, the fibril stress was given by

$$\sigma_f = -\frac{\eta}{2\sqrt{\left(\sigma_f - E_f^0\varepsilon_f\right)E_f^\varepsilon}}\dot{\sigma}_f + E_f^0\varepsilon_f + \left(\eta + \frac{\eta E_f^0}{2\sqrt{\left(\sigma_f - E_f^0\varepsilon_f\right)E_f^\varepsilon}}\right)\dot{\varepsilon}_f, \quad (1)$$

for $\varepsilon_f > 0$ (tension), where σ_f and ε_f represent the fibril stress and strain, respectively[20,21,38,39], and the mechanical properties of the viscoelastic fibrils were expressed with the initial fibril network modulus E_f^0, strain-dependent fibril network modulus E_f^ε, and damping coefficient η. The fibril stress was zero for: $\varepsilon_f \leq 0$ (compression).

The non-fibrillar matrix was modeled as a Neo-Hookean poroelastic material with the Young's modulus (E_{nf}), Poisson's ratio (ν) and permeability (k). The permeability was dependent on the void ratio as follows:

$$k=k_0\left(\frac{1+e}{1+e_0}\right)^M, \quad (2)$$

where k_0 is the initial permeability, M is the permeability strain-dependency factor end e and e_0 are current and initial void ratios, respectively. More details of the model and model validation can be found in earlier studies[20,21,38,39].

Cartilage thicknesses in the models were based on ultrasound measurements (Fig. 1). The finite element meshes consisted of 624 linear axisymmetric pore pressure continuum elements and the following boundary conditions were applied: cartilage edge and free surface were assumed to be fully permeable (zero pore pressure), contact between the indenter and cartilage was assumed to be impermeable, and cartilage-bone interface was fixed in all directions. At the axis of symmetry, lateral displacements were prevented and fluid was not allowed to flow through this boundary.

In order to obtain optimized material parameters for each sample, the FRPVE model was fitted to the experimental indentation tests by minimizing the mean absolute error (< 1 %) between the experimental and simulated reaction forces. The optimization of the parameters (E_f^0, E_f^ε, E_{nf}, k_0 and M) was conducted by using Matlab's built-in zero finding algorithm (Fig. 2) in combination with Abaqus. The rest of the material parameters (ν = 0.15 and η = 947 MPa s) were taken from the literature and kept constant[4,20,21,38].

1.1.1. MICROSCOPIC AND SPECTROSCOPIC METHODS

The samples fixed in formalin were processed for depth-dependent microscopic and spectroscopic analysis of tissue composition and structure. The collagen content was estimated with FTIRI (A Perkin Elmer Spotlight 300, Perkin Elmer, Shelton, CO, USA) by integration of the amide I region (1585 – 1720 cm^{-1}) (Fig. 2)[3,6,25,26]. PLM (Leitz Ortholux II POL, Leitz, Wetzlar, Germany) was used to analyze the collagen orientation angles (0° indicating the angle parallel to the cartilage surface) of the samples (Fig. 3) based on Stokes parameters[29,30]. The PG content was determined with DD from Safranin O [36] stained sections using CCD camera (SenSys, Photometrics Inc., Tucson, AZ, USA) mounted on a light microscope (Leitz Orthoplan, Leitz, Wetzlar, Germany)[27,28] (Fig. 4). After DD, the sections were used to determine the Mankin score of the samples[31,32]. Sample processing and microscopic and spectroscopic methods are presented more in detail in supplementary material.

1.1.2. STATISTICAL ANALYSIS

Linear correlation analysis (Pearson) was used to determine the relationships between the microscopic/spectroscopic parameters and model-derived mechanical parameters. The measured microscopic and spectroscopic parameters (PG content, collagen content and collagen orientation) were analyzed quantitatively for the superficial layer (5% of cartilage thickness) and for the entire tissue (100 % of cartilage thickness) that were then used in the correlation analyses.

RESULTS

The Mankin score of the samples varied from 2 to 11. Degeneration of the cartilage samples caused distinct depth-dependent alterations in all of the spectroscopic and microscopic

Europe PMC Funders Author Manuscripts

parameters (Figs. 2-4); lowering the collagen and PG content throughout tissue depth and increasing the collagen orientation angle (0° indicating the angle parallel to the cartilage surface) in the superficial and middle zones of the samples. Significant linear correlations were found between the Mankin score and all structural parameters of the superficial tissue; $r = -0.64$, $p = 0.010$ with the collagen content, $r = -0.55$, $p = 0.03$ with the PG content, $r = 0.58$, $p = 0.02$ with the collagen orientation and $r = -0.64$, $p = 0.011$ with the sample thickness.

The FRPVE model could successfully simulate the performed indentation tests with an average correlation coefficient of 0.99 and a mean absolute error of 0.5 % between the experimental and computational curves (Figs. 1C and 1D). The optimized material parameters of the FRPVE models, shown in Table 1, showed a large variation. Interestingly, the strain-dependent collagen fibril network modulus, E_f^e, was very low, at most 2 MPa. Low values of the fibril network and non-fibrillar matrix moduli and high permeabilities in highly degenerated samples caused lower and more homogenously distributed maximum principal stresses and pore pressures (Fig. 5).

Significant linear correlations were found between different FRPVE model and spectroscopic and microscopic parameters of the superficial tissue (Table 2, Fig. 6). Specifically, the strain-dependent fibril network modulus, E_f^e, exhibited a negative linear correlation with the collagen orientation angle ($r = -0.65$, $p = 0.009$) (Fig. 6A, Table 2), while the permeability strain-dependency factor, M, exhibited a positive linear correlation with the collagen content ($r = 0.56$, $p = 0.03$) (Table 2, Fig. 6B). The nonfibrillar matrix modulus, E_{nf}, also exhibited a positive linear correlation with the PG content ($r = 0.54$, $p = 0.04$) (Table 2).

DISCUSSION

This was the first study where the FRPVE model, mechanical testing, microscopic and spectroscopic techniques were combined to investigate the relationships between model-derived functional properties and structure of articular cartilage obtained from osteoarthritic human hip joints. Furthermore, the constituent specific (collagen, PGs, fluid) mechanical parameters were defined for the first time for osteoarthritic human cartilage. The most important findings indicated that, during the progression of OA, the reduced collagen content altered fluid flow and pressurization of cartilage in a depth-dependent manner, while the increased collagen orientation angle (0° indicating the angle parallel to the cartilage surface) impaired the strain-dependent collagen fibril and tensile stiffness of the tissue.

One of the most interesting results was the positive correlation between the collagen content and the permeability strain-dependency factor (M). This suggests that dense packing of the collagen fibrils impairs the fluid flow out from the tissue during tissue compression, reducing the permeability faster as a function of strain in the normal samples with more collagen[4,21,40]. On the other hand, M approached zero in severely osteoarthritic samples, indicating that due to the loose packing of the collagen, fluid flow out from the tissue was not affected by compressive strain. This further suggests that the nonlinear response of cartilage to loading and increase in resistance to instantaneous loading as a function of strain (as a result of nonlinear permeability and subsequent increase in fluid pressure) is much weaker in OA cartilage than normal, healthy tissue in a hip joint. An implication of this might be that weakened articular cartilage collagen impairs the ability of cartilage for fluid pressurization and fluid load support[41], which leads to a weakened tissue response under impact loading and may accelerate the progression of OA. Increased compressive strains could also lead to increased cell death and damage in deeper layers of cartilage as well as in the cartilage-bone interface and subchondral bone.

Consistent with former observations[4,21,42], the PG content correlated positively and significantly with the nonfibrillar matrix modulus, E_{nf}. This supports earlier studies which indicate that PGs contribute considerably to the compressive strength of the tissue, *i.e.* low values of the nonfibrillar matrix modulus were indicative of the reduced PG content in OA cartilage.

The strain-dependent collagen network modulus, E_f^{ε}, correlated negatively with the collagen orientation angle (0° indicating the angle parallel to the cartilage surface), but no correlation could be found between E_f^{ε} and the collagen content. This indicates that fibrillation of the superficial zone collagens or wear during OA are much more dominant factors than is the collagen content to modulate the tensile stiffness of cartilage. When the tangentially oriented collagens fibrillate and lose their organization, the stiffness of the collagen fibril network is reduced and cartilage loses its ability to resist tensile stresses. This is specifically accentuated with increasing strain, as indicated by E_f^{ε}. Then in turn, an even greater amount of collagen would have no significant influence on the fibril network stiffness in tangential direction under subsequential loadings.

The literature is lacking the information of the fibril reinforced biphasic mechanical properties of human OA articular cartilage, especially those for a hip joint. The initial permeability k_0, permeability strain-dependency factor M, initial collagen network modulus E_f^0 and nonfibrillar matrix modulus E_{nf} obtained from this study were in agreement with previous studies conducted for bovine[4,17,21,43] and ovine[24] cartilage. However, the strain-dependent collagen network modulus, E_f^0, was very low (Table 1). In other studies, the values have been two to three orders of magnitude higher[4,21,39,43]. In healthy cartilage, the collagen fibril network stiffening, nonlinear stress-strain response and increase in the dynamic modulus (as a function of strain) is well documented[20,43,44]. In the present study, the samples with high Mankin scores and fibrillated collagen experienced almost negligible tensile stiffening, *i.e.*, the E_f^{ε} was close to zero. The samples that were relatively healthy (Mankin score 2) which also contained all the other material parameters close to the literature values, still had low values of E_f^{ε}. This suggests that collagen straightening, that has traditionally been suggested to cause tensile stiffening in many soft tissues[45,46], is not that important phenomenon in osteoarthritic human hip cartilage. It is also possible that relatively healthy tissue had straightened collagen fibrils already at rest, which is supported by a thick layer of tangentially oriented fibrils in the superficial tissue (Fig. 3). Since indentation is controlled primarily by the superficial layers, tissue compression may have caused a linear stress-strain response and an almost constant, strain-independent fibril network modulus.

Indentation testing was chosen because the technique is highly sensitive to reveal alterations in the properties of the superficial layers of cartilage. This was supported by the present results in which the structural parameters determined for the superficial tissue (5% of cartilage thickness) correlated significantly with the mechanical properties of the tissue. The most distinguishable structural parameter was the collagen orientation angle, which changed only in the superficial/intermediate tissue layers during the progression of OA (Fig. 3). Similar findings for the collagen orientation angle have been demonstrated earlier[3,47]. Structure-function relationships were also analyzed with the structural values calculated for the entire tissue thickness. In those analyses, all significant correlations disappeared. This supports the importance of the superficial cartilage layer on indentation response, as also shown before[48,49].

The FRPVE model successfully simulated the experimental indentation tests (the mean absolute error between the model and experiment was 0.5 %). Every optimized parameter had a different influence on the stress-relaxation response and the optimization process was

performed with different initial values, but produced the same results. A parametric analysis of the effect of the model parameters has also been shown earlier, and the same parameters as optimized here have also been successfully optimized in earlier studies[20,21]. Thus, we believe that unique material parameters were obtained from each optimization.

Uniqueness in the determination of the optimized material parameters was further assured by taking the damping coefficient of the collagen fibrils directly from the literature[4,20,21]. The same parameter was also fixed in an earlier study in which the FRPVE model was fitted to the experimental stress-relaxation responses of healthy bovine cartilage[21]. However, as there is no information about the damping coefficient of the fibrils (η) for human cartilage, this means that our chosen value could be inaccurate. In order to assure ourselves on the accuracy of the value for η that we selected, we tested the effect of the damping coefficient on the optimized values of material parameters, especially concentrating on the low values of the strain-dependent collagen network modulus E_f^{ε}. Depending on the sample, changing η by one order of magnitude could approximately double E_f^{ε}, leaving it still very low.

Another parameter that was kept constant for assuring the uniqueness of the material parameters was the Poisson's ratio. In the FRPVE model the Poisson's ratio represents only the non-fibrillar matrix[20], while the effective Poisson's ratio of the whole cartilage tissue is strongly controlled by the stiffness of the collagen network in the model[50-53]. The chosen value of 0.15 has been used before in the FRPVE modeling studies[20], and sensitivity test showed that variations between 0.05 and 0.25 did not have substantial effect on the model result.

In order to keep the structural analysis independent of the biomechanical analysis, the depth-dependent properties of the cartilage, *e.g.*, collagen or PGs, were not implemented in the FE model. Sample specific structural properties could have affected the optimized material parameters. We tested the depth-dependent collagen orientation on the model response. By implementing the collagen orientation in the superficial, middle and deep zones as parallel to the cartilage surface, random, and perpendicular to the cartilage surface, respectively, E_f^{ε} could be about ten times bigger than presented in Table 1. This value would be comparable with healthy bovine tibial cartilage (24 MPa)[21], which is known to be less stiff under impact or dynamic loading. However, as mentioned before, the depth-dependent collagen orientation, collagen content and PG content were not implemented in the models because they would have made the modeling analysis dependent on the structural analysis. Now, all the analyses were independent of each other, making the correlation analysis reasonable. For the analysis of the mechanical response of cartilage solely based on tissue structure and composition, as has been done recently[35,58], implementation of the collagen and PG distributions and amounts would become necessary.

For this study, we did not measure the mechanical behaviour of cartilage in a depth-dependent manner. Instead, the goal of this study was to characterize the fibril reinforced poroelastic material properties for osteoarthritic human cartilage and investigate their relationships with tissue structure and composition. Indentation is also possible to conduct for diagnostical purposes and here it clearly indicated with the model certain structural changes in OA, especially those in the superficial tissue layers. In the future, it would be interesting to measure local tissue strains and stresses of diseased cartilage and compare those to the depth-dependent tissue structure and composition[50,54-57].

There has been debate about scoring systems, specifically in terms of their reproducibility and the validity of the Mankin scoring for OA cartilage has been questioned[59,60], and the OARSI scoring system has been proposed to be a more valid tool[61]. Here Mankin scores correlated significantly with all structural parameters. Safranin O staining is a part of the

scoring, so the PG content and Mankin score correlation is obvious. However, larger Mankin scores of the tissue were consistent with a decrease in the collagen content, a modification in collagen orientation as well as a loss of cartilage thickness, supporting the use and validity of this scoring system.

One limitation in the present study was the potential escape of PGs through the surfaces of the samples during DMEM incubation. However, the PG content in the superficial tissue with respect to the deep tissue across all samples were consistent with earlier studies where human osteoarthritic cartilage samples have been used[3,6,62]. This indicates that possible PG loss was minimal. Another limitation was that even though the relaxation time was based on our preliminary tests and the literature[21,35-37], the full equilibrium was not reached in higher strains for a few samples with low Mankin scores (*e.g.* Fig. 1C). Despite this, the FRPVE-model simulated all of the experimental stress-relaxation tests, and the modeling results should not depend on whether the plateau was fully reached.

Negative correlation between the Mankin score and sample thickness indicates cartilage wear. Cartilage thickness changed from 2.3 mm to 0.5 mm with the increase of Mankin score from 2 to 11. Wear of the superficial/middle tissue is supported by the loss of the tangentially oriented collagen fibrils (Fig. 3). Changes in the collagen fibril orientation angle in the superficial tissue and superficial zone thickness have also been observed earlier[3,63] in severely degenerated human patellar cartilage. However, the average values of sample thicknesses in Saarakkala et al. (2010)[3] in normal and advanced OA group were almost the same, 2.6 and 2.9 mm, respectively. Since the division of the samples in groups was different in the aforementioned earlier studies and in the present study and due to the use of different scoring systems, tissue thicknesses can't be compared directly. On the other hand, this could indicate different cartilage wear in knee and hip joints.

Even though the number of samples was low (9 patients, $n = 15$) and there were no normal cartilage, the randomness in collection of the samples enabled large variation in the properties of the samples. Intra-class correlation was insignificant for all the structural and mechanical parameters, suggesting that cartilage properties were not patient-specific. Only two patients had similar structural and mechanical parameters. However, this did not have an effect on the conclusions of this study (*i.e.* by removing the other data points of patients did not change the conclusions). This was desirable since the samples were neither used to represent patients nor to compare between diseased and normal cartilage, but to find out how the structural properties modulate the model-derived functional properties of OA cartilage.

The present study demonstrated the capability of the FRPVE model in combination with microscopic and spectroscopic methods to characterize the structure-function relationships of osteoarthritic human hip joint articular cartilage. The collagen content and orientation as well as the PG content of the superficial tissue were shown to modulate the strain- and depth-dependent functional properties of osteoarthritic cartilage in their own distinct manners. Thus, the results provide important and specific information of the strain- and depth-dependent structure-function relationships of human cartilage and mechanisms during the progression of OA in the hip joint.

Supplementary Material

Refer to Web version on PubMed Central for supplementary material.

Acknowledgments

Financial support from Academy of Finland (grants no. 140730 and 218038); Kuopio University Hospital (EVO 15283); European Research Council (ERC 281180); and Sigrid Juselius Foundation are acknowledged. CSC-IT

Center for Science, Finland, Mr. Mika Mikkola, M.Sc., and Mr. Mika Mononen, M.Sc., are acknowledged for technical support. Dr. Santtu Mikkonen, Ph.D., is acknowledged for statistical assistance and Dr. James Fick, Ph.D., for the English review.

REFERENCES

1. Mow, VC.; Hayes, WC. Basic Orthopaedic Biomechanics. Raven Press, Ltd; New York: 1991.
2. Arokoski JP, Jurvelin JS, Vaatainen U, Helminen HJ. Normal and pathological adaptations of articular cartilage to joint loading. Scand.J.Med.Sci.Sports. 2000; 10:186–98. [PubMed: 10898262]
3. Saarakkala S, Julkunen P, Kiviranta P, Makitalo J, Jurvelin JS, Korhonen RK. Depth-wise progression of osteoarthritis in human articular cartilage: investigation of composition, structure and biomechanics. Osteoarthritis Cartilage. 2010; 18:73–81. [PubMed: 19733642]
4. Korhonen RK, Laasanen MS, Toyras J, Lappalainen R, Helminen HJ, Jurvelin JS. Fibril reinforced poroelastic model predicts specifically mechanical behavior of normal, proteoglycan depleted and collagen degraded articular cartilage. J.Biomech. 2003; 36:1373–9. [PubMed: 12893046]
5. Buckwalter JA, Mankin HJ. Articular cartilage: degeneration and osteoarthritis, repair, regeneration, and transplantation. Instr.Course Lect. 1998; 47:487–504. [PubMed: 9571450]
6. Bi X, Yang X, Bostrom MP, Camacho NP. Fourier transform infrared imaging spectroscopy investigations in the pathogenesis and repair of cartilage. Biochim.Biophys.Acta. 2006; 1758:934–41. [PubMed: 16815242]
7. Panula HE, Hyttinen MM, Arokoski JP, Langsjo TK, Pelttari A, Kiviranta I, et al. Articular cartilage superficial zone collagen birefringence reduced and cartilage thickness increased before surface fibrillation in experimental osteoarthritis. Ann.Rheum.Dis. 1998; 57:237–45. [PubMed: 9709181]
8. Bi X, Li G, Doty SB, Camacho NP. A novel method for determination of collagen orientation in cartilage by Fourier transform infrared imaging spectroscopy (FT-IRIS). Osteoarthritis Cartilage. 2005; 13:1050–8. [PubMed: 16154778]
9. Armstrong CG, Mow VC. Variations in the intrinsic mechanical properties of human articular cartilage with age, degeneration, and water content. J.Bone Joint Surg.Am. 1982; 64:88–94. [PubMed: 7054208]
10. Altman RD, Dean DD. Osteoarthritis research: animal models. Semin.Arthritis Rheum. 1990; 19:21–5. [PubMed: 2180067]
11. Bendele A, McComb J, Gould T, McAbee T, Sennello G, Chlipala E, et al. Animal models of arthritis: relevance to human disease. Toxicol.Pathol. 1999; 27:134–42. [PubMed: 10367688]
12. Bendele AM. Animal models of osteoarthritis. J.Musculoskelet.Neuronal Interact. 2001; 1:363–76. [PubMed: 15758487]
13. LeRoux MA, Arokoski J, Vail TP, Guilak F, Hyttinen MM, Kiviranta I, et al. Simultaneous changes in the mechanical properties, quantitative collagen organization, and proteoglycan concentration of articular cartilage following canine meniscectomy. J.Orthop.Res. 2000; 18:383–92. [PubMed: 10937624]
14. Nieminen MT, Toyras J, Rieppo J, Hakumaki JM, Silvennoinen J, Helminen HJ, et al. Quantitative MR microscopy of enzymatically degraded articular cartilage. Magn.Reson.Med. 2000; 43:676–81. [PubMed: 10800032]
15. Canal Guterl C, Hung CT, Ateshian GA. Electrostatic and non-electrostatic contributions of proteoglycans to the compressive equilibrium modulus of bovine articular cartilage. J.Biomech. 2010; 43:1343–50. [PubMed: 20189179]
16. Cohen B, Lai WM, Mow VC. A transversely isotropic biphasic model for unconfined compression of growth plate and chondroepiphysis. J.Biomech.Eng. 1998; 120:491–6. [PubMed: 10412420]
17. DiSilvestro MR, Zhu Q, Wong M, Jurvelin JS, Suh JK. Biphasic poroviscoelastic simulation of the unconfined compression of articular cartilage: I--Simultaneous prediction of reaction force and lateral displacement. J.Biomech.Eng. 2001; 123:191–7. [PubMed: 11340881]
18. Li LP, Soulhat J, Buschmann MD, Shirazi-Adl A. Nonlinear analysis of cartilage in unconfined ramp compression using a fibril reinforced poroelastic model. Clin.Biomech. (Bristol, Avon). 1999; 14:673–82.

19. Soltz MA, Ateshian GA. A Conewise Linear Elasticity mixture model for the analysis of tension-compression nonlinearity in articular cartilage. J.Biomech.Eng. 2000; 122:576–86. [PubMed: 11192377]
20. Wilson W, van Donkelaar CC, van Rietbergen B, Ito K, Huiskes R. Stresses in the local collagen network of articular cartilage: a poroviscoelastic fibril-reinforced finite element study. J.Biomech. 2004; 37:357–66. [PubMed: 14757455]
21. Julkunen P, Kiviranta P, Wilson W, Jurvelin JS, Korhonen RK. Characterization of articular cartilage by combining microscopic analysis with a fibril-reinforced finite-element model. J.Biomech. 2007; 40:1862–70. [PubMed: 17052722]
22. Li LP, Buschmann MD, Shirazi-Adl A. A fibril reinforced nonhomogeneous poroelastic model for articular cartilage: inhomogeneous response in unconfined compression. J.Biomech. 2000; 33:1533–41. [PubMed: 11006376]
23. Li LP, Herzog W, Korhonen RK, Jurvelin JS. The role of viscoelasticity of collagen fibers in articular cartilage: axial tension versus compression. Med.Eng.Phys. 2005; 27:51–7. [PubMed: 15604004]
24. Seifzadeh A, Wang J, Oguamanam DC, Papini M. A nonlinear biphasic fiber-reinforced porohyperviscoelastic model of articular cartilage incorporating fiber reorientation and dispersion. J.Biomech.Eng. 2011; 133:081004. [PubMed: 21950897]
25. Boskey A, Pleshko Camacho N. FT-IR imaging of native and tissue-engineered bone and cartilage. Biomaterials. 2007; 28:2465–78. [PubMed: 17175021]
26. Camacho NP, West P, Torzilli PA, Mendelsohn R. FTIR microscopic imaging of collagen and proteoglycan in bovine cartilage. Biopolymers. 2001; 62:1–8. [PubMed: 11135186]
27. Kiraly K, Lapvetelainen T, Arokoski J, Torronen K, Modis L, Kiviranta I, et al. Application of selected cationic dyes for the semiquantitative estimation of glycosaminoglycans in histological sections of articular cartilage by microspectrophotometry. Histochem.J. 1996; 28:577–90. [PubMed: 8894661]
28. Kiviranta I, Jurvelin J, Tammi M, Saamanen AM, Helminen HJ. Microspectrophotometric quantitation of glycosaminoglycans in articular cartilage sections stained with Safranin O. Histochemistry. 1985; 82:249–55. [PubMed: 2581923]
29. Rieppo J, Hallikainen J, Jurvelin JS, Kiviranta I, Helminen HJ, Hyttinen MM. Practical considerations in the use of polarized light microscopy in the analysis of the collagen network in articular cartilage. Microsc.Res.Tech. 2008; 71:279–87. [PubMed: 18072283]
30. Rieppo J, Hyttinen MM, Halmesmaki E, Ruotsalainen H, Vasara A, Kiviranta I, et al. Changes in spatial collagen content and collagen network architecture in porcine articular cartilage during growth and maturation. Osteoarthritis Cartilage. 2009; 17:448–55. [PubMed: 18849174]
31. Mankin HJ, Lippiello L. Biochemical and metabolic abnormalities in articular cartilage from osteo-arthritic human hips. J.Bone Joint Surg.Am. 1970; 52:424–34. [PubMed: 4246573]
32. Mankin HJ, Dorfman H, Lippiello L, Zarins A. Biochemical and metabolic abnormalities in articular cartilage from osteo-arthritic human hips. II. Correlation of morphology with biochemical and metabolic data. J.Bone Joint Surg.Am. 1971; 53:523–37. [PubMed: 5580011]
33. Toyras J, Laasanen MS, Saarakkala S, Lammi MJ, Rieppo J, Kurkijarvi J, et al. Speed of sound in normal and degenerated bovine articular cartilage. Ultrasound Med.Biol. 2003; 29:447–54. [PubMed: 12706196]
34. Huang YP, Zheng YP. Intravascular Ultrasound (IVUS): A Potential Arthroscopic Tool for Quantitative Assessment of Articular Cartilage. Open Biomed.Eng.J. 2009; 3:13–20. [PubMed: 19662152]
35. Julkunen P, Wilson W, Jurvelin JS, Rieppo J, Qu CJ, Lammi MJ, et al. Stress-relaxation of human patellar articular cartilage in unconfined compression: prediction of mechanical response by tissue composition and structure. J.Biomech. 2008; 41:1978–86. [PubMed: 18490021]
36. Korhonen RK, Laasanen MS, Toyras J, Rieppo J, Hirvonen J, Helminen HJ, et al. Comparison of the equilibrium response of articular cartilage in unconfined compression, confined compression and indentation. J.Biomech. 2002; 35:903–9. [PubMed: 12052392]

37. DiSilvestro MR, Suh JK. A cross-validation of the biphasic poroviscoelastic model of articular cartilage in unconfined compression, indentation, and confined compression. J.Biomech. 2001; 34:519–25. [PubMed: 11266676]
38. Wilson W, van Donkelaar CC, van Rietbergen B, Ito K, Huiskes R. J.Biomech. 2005; 38:2138–40. Erratum to “Stresses in the local collagen network of articular cartilage: a poroviscoelastic fibril-reinforced finite element study” [Journal of Biomechanics 37 (2004) 357-366] and “A fibril-reinforced poroviscoelastic swelling model for articular cartilage” [Journal of Biomechanics 38 (2005) 1195-1204].
39. Julkunen P, Korhonen RK, Herzog W, Jurvelin JS. Uncertainties in indentation testing of articular cartilage: a fibril-reinforced poroviscoelastic study. Med.Eng.Phys. 2008; 30:506–15. [PubMed: 17629536]
40. Maroudas A, Bullough P, Swanson SA, Freeman MA. The permeability of articular cartilage. J.Bone Joint Surg.Br. 1968; 50:166–77. [PubMed: 5641590]
41. Ateshian GA. The role of interstitial fluid pressurization in articular cartilage lubrication. J.Biomech. 2009; 42:1163–76. [PubMed: 19464689]
42. Schmidt MB, Mow VC, Chun LE, Eyre DR. Effects of proteoglycan extraction on the tensile behavior of articular cartilage. J.Orthop.Res. 1990; 8:353–63. [PubMed: 2324854]
43. Li LP, Buschmann MD, Shirazi-Adl A. Strain-rate dependent stiffness of articular cartilage in unconfined compression. J.Biomech.Eng. 2003; 125:161–8. [PubMed: 12751277]
44. Korhonen RK, Jurvelin JS. Compressive and tensile properties of articular cartilage in axial loading are modulated differently by osmotic environment. Med.Eng.Phys. 2010; 32:155–60. [PubMed: 19955010]
45. Roth V, Mow VC. The intrinsic tensile behavior of the matrix of bovine articular cartilage and its variation with age. J.Bone Joint Surg.Am. 1980; 62:1102–17. [PubMed: 7430196]
46. Woo SL, Akeson WH, Jemmott GF. Measurements of nonhomogeneous, directional mechanical properties of articular cartilage in tension. J.Biomech. 1976; 9:785–91. [PubMed: 1022791]
47. Changoor A, Nelea M, Methot S, Tran-Khanh N, Chevrier A, Restrepo A, et al. Structural characteristics of the collagen network in human normal, degraded and repair articular cartilages observed in polarized light and scanning electron microscopies. Osteoarthritis Cartilage. 2011; 19:1458–68. [PubMed: 22015933]
48. Korhonen RK, Wong M, Arokoski J, Lindgren R, Helminen HJ, Hunziker EB, et al. Importance of the superficial tissue layer for the indentation stiffness of articular cartilage. Med.Eng.Phys. 2002; 24:99–108. [PubMed: 11886828]
49. Julkunen P, Jurvelin JS, Isaksson H. Contribution of tissue composition and structure to mechanical response of articular cartilage under different loading geometries and strain rates. Biomech.Model.Mechanobiol. 2010; 9:237–45. [PubMed: 19680701]
50. Jurvelin JS, Buschmann MD, Hunziker EB. Optical and mechanical determination of Poisson’s ratio of adult bovine humeral articular cartilage. J.Biomech. 1997; 30:235–41. [PubMed: 9119822]
51. Athanasiou KA, Agarwal A, Muffoletto A, Dzida FJ, Constantinides G, Clem M. Biomechanical properties of hip cartilage in experimental animal models. Clin.Orthop.Relat.Res. 1995; (316): 254–66. [PubMed: 7634715]
52. Athanasiou KA, Agarwal A, Dzida FJ. Comparative study of the intrinsic mechanical properties of the human acetabular and femoral head cartilage. J.Orthop.Res. 1994; 12:340–9. [PubMed: 8207587]
53. Kiviranta P, Rieppo J, Korhonen RK, Julkunen P, Toyras J, Jurvelin JS. Collagen network primarily controls Poisson’s ratio of bovine articular cartilage in compression. J.Orthop.Res. 2006; 24:690–9. [PubMed: 16514661]
54. Schinagl RM, Gurskis D, Chen AC, Sah RL. Depth-dependent confined compression modulus of full-thickness bovine articular cartilage. J.Orthop.Res. 1997; 15:499–506. [PubMed: 9379258]
55. Chen SS, Falcovitz YH, Schneiderman R, Maroudas A, Sah RL. Depth-dependent compressive properties of normal aged human femoral head articular cartilage: relationship to fixed charge density. Osteoarthritis Cartilage. 2001; 9:561–9. [PubMed: 11520170]

56. Chen AC, Bae WC, Schinagl RM, Sah RL. Depth- and strain-dependent mechanical and electromechanical properties of full-thickness bovine articular cartilage in confined compression. J.Biomech. 2001; 34:1–12. [PubMed: 11425068]
57. Guilak F, Ratcliffe A, Mow VC. Chondrocyte deformation and local tissue strain in articular cartilage: a confocal microscopy study. J.Orthop.Res. 1995; 13:410–21. [PubMed: 7602402]
58. Wilson W, Huyghe JM, van Donkelaar CC. A composition-based cartilage model for the assessment of compositional changes during cartilage damage and adaptation. Osteoarthritis Cartilage. 2006; 14:554–60. [PubMed: 16476555]
59. Ostergaard K, Petersen J, Andersen CB, Bendtzen K, Salter DM. Histologic/histochemical grading system for osteoarthritic articular cartilage: reproducibility and validity. Arthritis Rheum. 1997; 40:1766–71. [PubMed: 9336409]
60. Ostergaard K, Andersen CB, Petersen J, Bendtzen K, Salter DM. Validity of histopathological grading of articular cartilage from osteoarthritic knee joints. Ann.Rheum.Dis. 1999; 58:208–13. [PubMed: 10364898]
61. Pritzker KP, Gay S, Jimenez SA, Ostergaard K, Pelletier JP, Revell PA, et al. Osteoarthritis cartilage histopathology: grading and staging. Osteoarthritis Cartilage. 2006; 14:13–29. [PubMed: 16242352]
62. David-Vaudey E, Burghardt A, Keshari K, Brouchet A, Ries M, Majumdar S. Fourier Transform Infrared Imaging of focal lesions in human osteoarthritic cartilage. Eur.Cell.Mater. 2005; 10:51, 60. discussion 60. [PubMed: 16307426]
63. Saarakkala S, Julkunen P. Specifity of Fourier Transform Infrared (FTIR) Microspectroscopy to Estimate Depth-Wise Proteoglycan Content in Normal and Osteoarthritic. Human Articular Cartilage. 2010; 1:262–269.

Europe PMC Funders Author Manuscripts

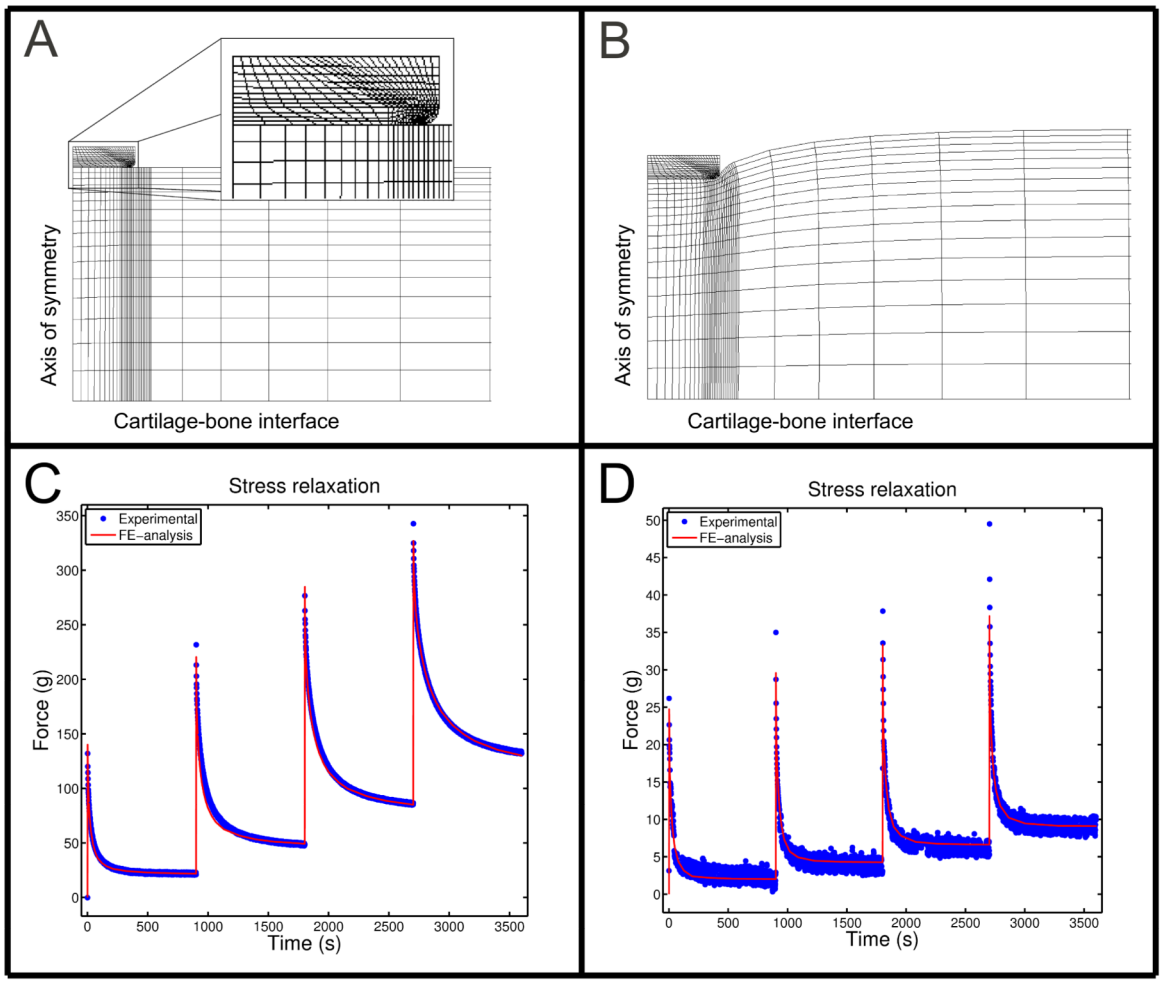

Figure 1.

A section of the finite element mesh from a cartilage sample of 2.3 mm in thickness A) before loading ($t = 0$ s) and B) at the end of the relaxation test ($t = 3600$ s), and experimental stress-relaxation responses and the optimized model predictions for two different samples with Mankin scores of C) 2.4 and D) 8.6.

Europe PMC Funders Author Manuscripts

Europe PMC Funders Author Manuscripts

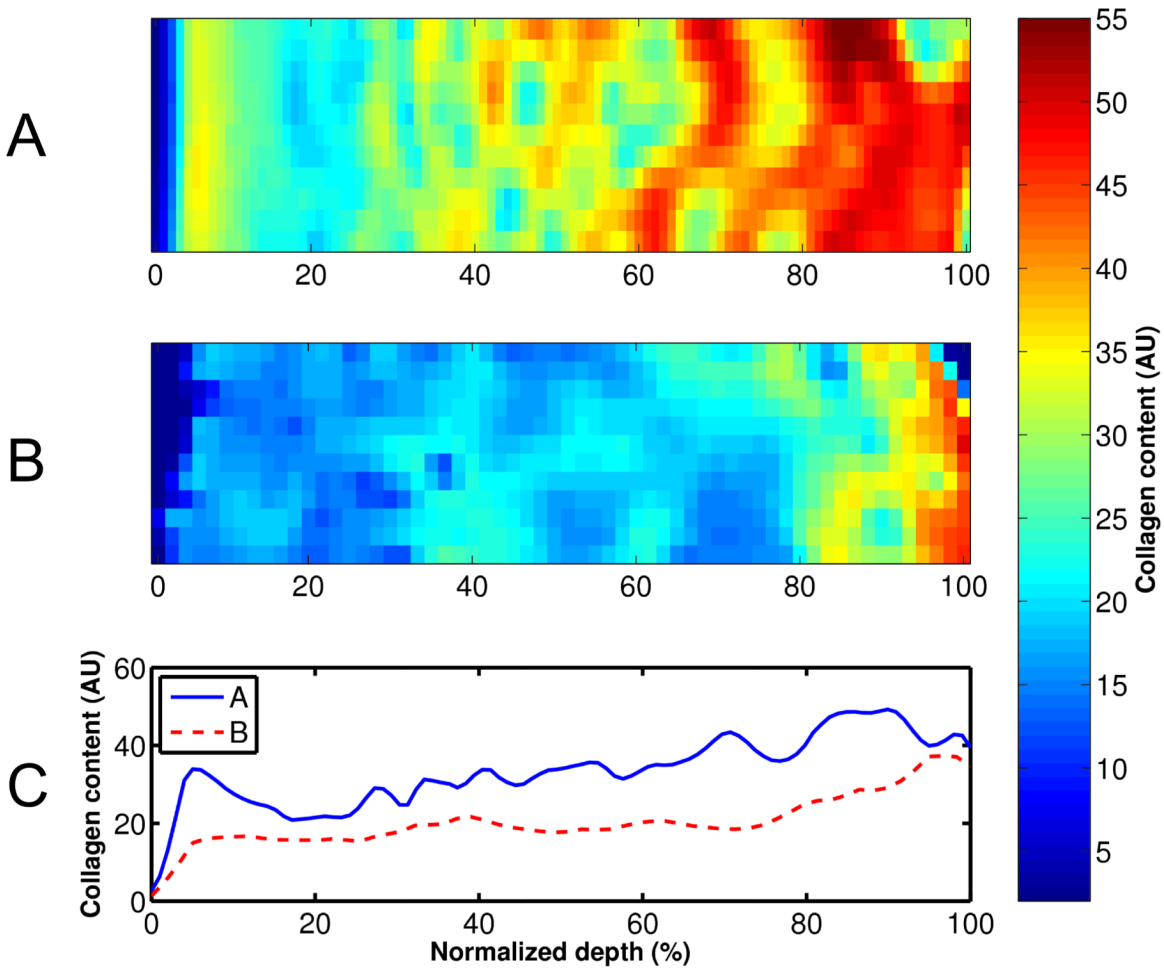

Figure 2.
Amide I absorption maps (A, B) and profiles (C), *i.e.*, an estimation of the collagen content, measured with FTIRI. Mankin scores of the samples were (A) 2.4 and (B) 8.6.

Europe PMC Funders Author Manuscripts

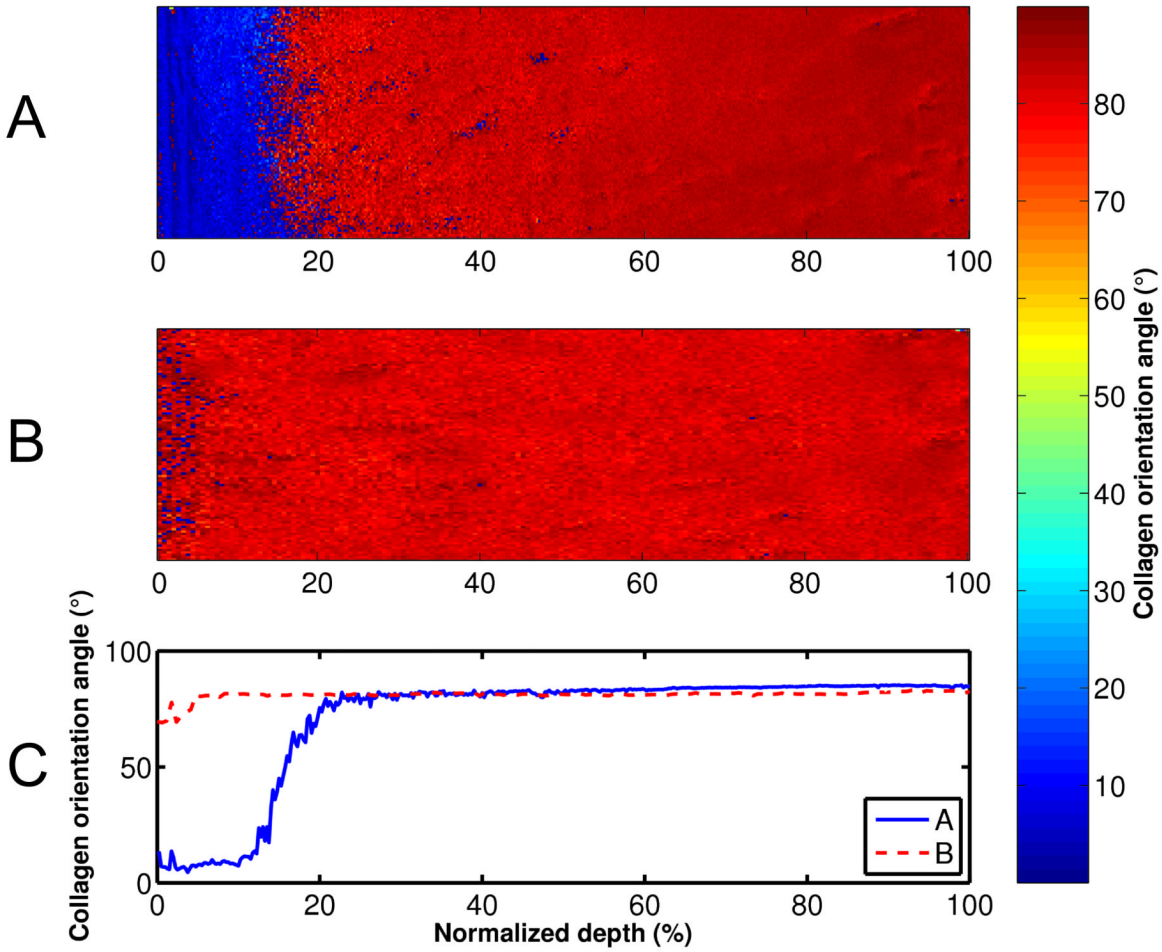

Figure 3.
Collagen orientation angle maps (A, B) and profiles (C), measured with PLM. Mankin scores of the samples were (A) 2.4 and (B) 8.6.

Europe PMC Funders Author Manuscripts

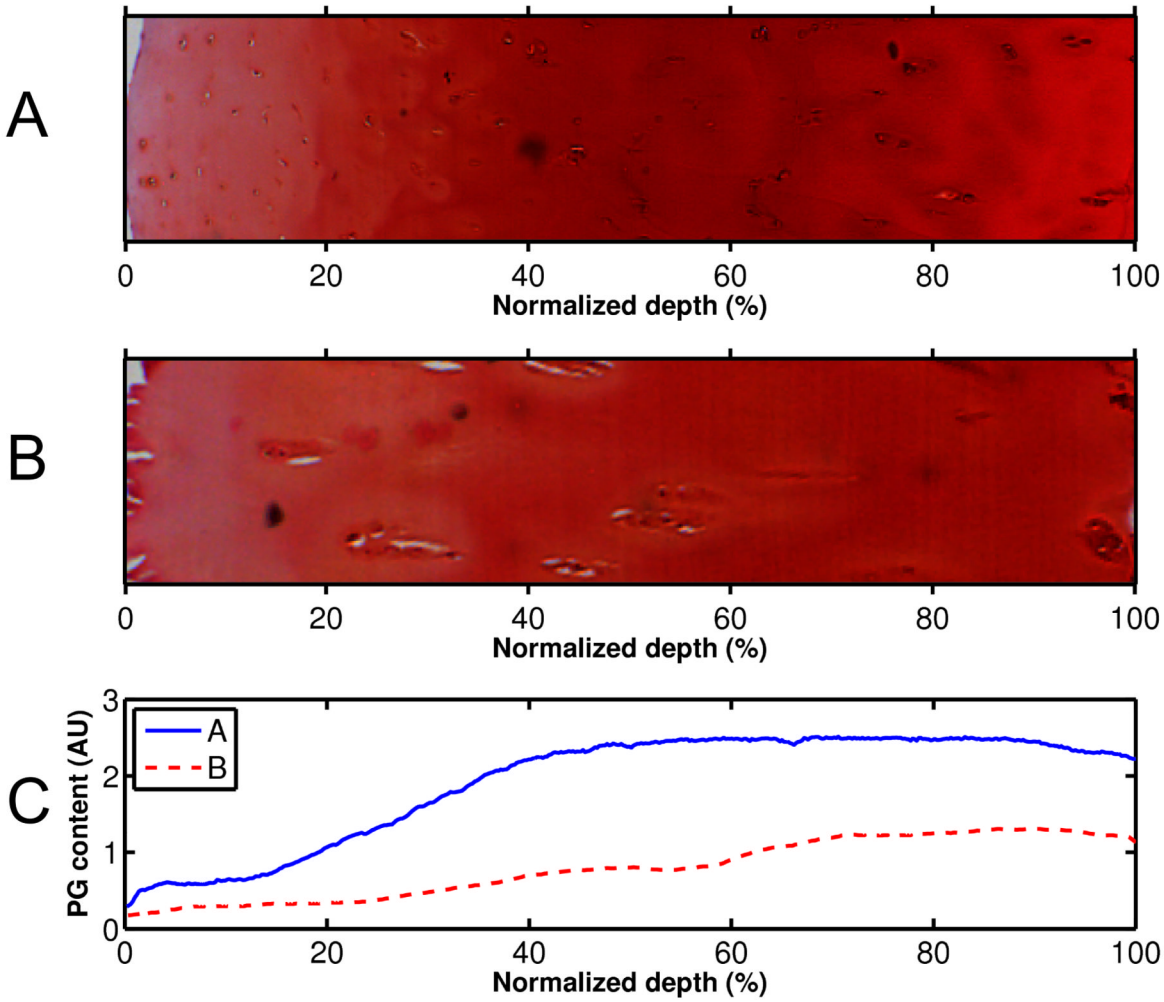

Figure 4.

Microscopy images (A, B) and profiles (C) of safranin O stained sections, *i.e.*, estimate of the proteglycan content, measured with DD. Mankin scores of the samples were (A) 2.4 and (B) 8.6.

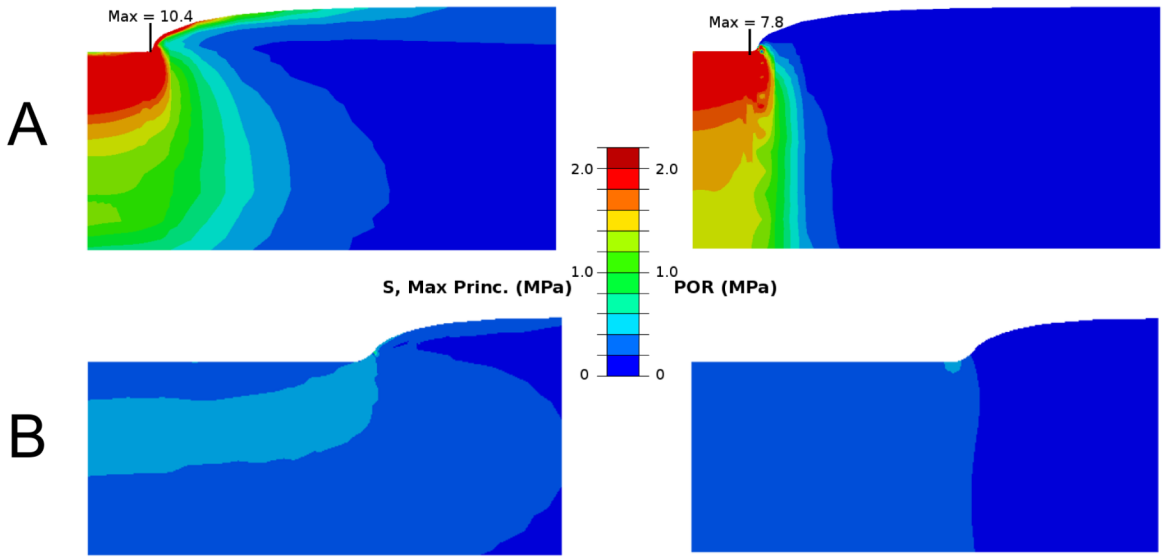

Figure 5.
Maximum principal stress (left) and pore pressure (right) distributions in two cartilage samples. Mankin scores of the samples were (A) 2.4 and (B) 8.6. The distributions were analyzed from the beginning of the fourth or last stress-relaxation period. For clarity, the figures have different size scales.

Europe PMC Funders Author Manuscripts

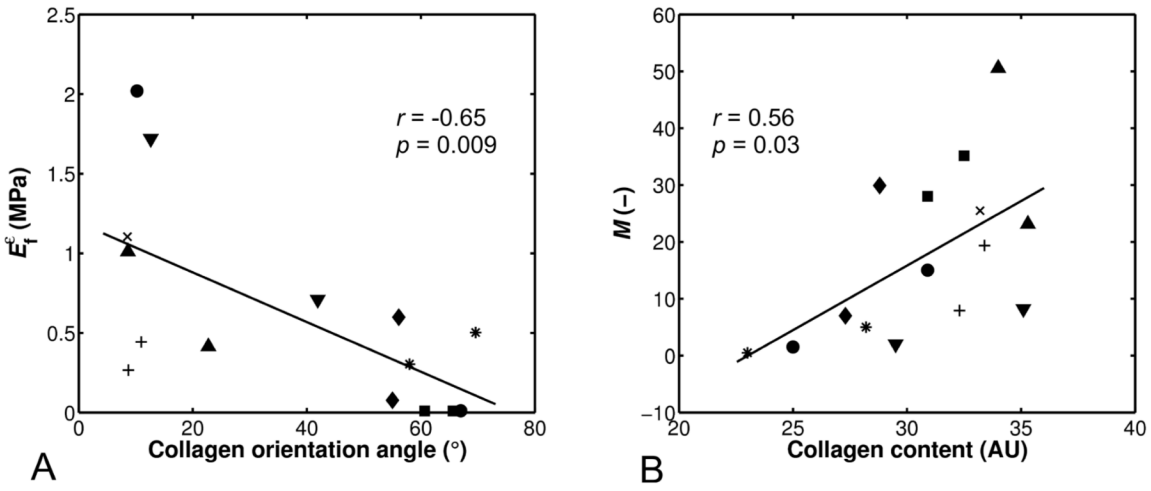

Figure 6.

Linear correlations between (A) the strain-dependent collagen network modulus (E_f^{ε}) and the collagen orientation angle of the superficial tissue layer, and (B) the permeability strain-dependency factor (M) and the collagen content of the superficial tissue layer. The samples from the same patient are marked with the same symbols.

Europe PMC Funders Author Manuscripts

Europe PMC Funders Author Manuscripts

Table 1

Values (maximum, minimum, mean and standard deviation) for the optimized material parameters

	E_f^0 (MPa)	E_f^e (MPa)	E_{nf} (MPa)	k_0 (10^{-15}m^4/Ns)	M
max	1.95	2.02	0.90	10.98	50.54
mean±std	0.59±0.48	0.61±0.61	0.23±0.22	3.66±2.86	17.26±14.64
min	0.03	0.01	0.02	0.82	0.50

E_f^0 is the initial collagen network modulus, E_f^e the strain-dependent collagen network modulus, E_{nf} the nonfibrillar matrix modulus, k_0 the initial permeability and M the permeability strain-dependency factor.

Europe PMC Funders Author Manuscripts

Table 2

Linear correlation coefficients between the structural (superficial layer, 5% of cartilage thickness) and mechanical parameters

	E_f^0	E_f^e	E_{nf}	k_0	M
Collagen content	0.33	0.16	0.28	0.10	0.56*
PG content	0.38	0.01	0.54*	−0.19	0.23
Collagen orientation	−0.20	−0.65**	−0.22	−0.03	−0.23

E_f^0 is the initial collagen network modulus, E_f^e the strain-dependent collagen network modulus, E_{nf} the nonfibrillar matrix modulus, k_0 the initial permeability and M the permeability strain-dependency factor.

* $p < 0.05$

** $p < 0.01$